

RUSSIAN ACADEMY OF SCIENCE
Lenin Order of Siberian Branch
G.I. BUDKER INSTITUTE OF NUCLEAR PHYSICS

V.N. Baier and V.M. Katkov

ELECTROPRODUCTION
OF ELECTRON-POSITRON PAIR
IN ORIENTED CRYSTAL
AT HIGH ENERGY

Budker INP 2008-28

Novosibirsk
2008

Electroproduction of electron-positron pair in oriented crystal at high energy

V.N. Baier and V.M. Katkov

Institute of Nuclear Physics
630090, Novosibirsk, Russia

Abstract

The process of electroproduction of the electron-positron pair by high energy electron in an oriented single crystal is investigated. Two contributions are considered: the direct (one-step) process via the virtual intermediate photon and the cascade(two-step) process when the electron emits the real photon moving in the field of axis and afterwards the photon converts into the pair. The spectrum of created positron(electron) is found. It is shown that the probability of the process is strongly enhanced comparing with the corresponding amorphous medium.

1 Introduction

The photon emission from high energy electron and electron-positron pair creation by a photon are the basic electrodynamics processes in oriented crystal at high energy. The probabilities of these processes are strongly enhanced comparing with the corresponding amorphous medium [1]. The photon emitted by electron can produce the electron-positron pair (the electroproduction or the trident production process). An analysis of this process is of evident interest as example of higher order QED process in an oriented crystal. This process is the first step of the electromagnetic cascade developed in a crystal by the incident electron (the cascade processes in oriented crystals was considered in [2], see also Sec.20 in [1]), it possesses many important peculiarities which will be discussed below.

Recently authors developed a new approach to analysis of pair creation by a photon [3] and radiation from high energy electrons [4] in oriented crystals . This approach permits to consider simultaneously both the coherent and incoherent mechanisms of these processes. For calculation of the energy spectrum of created particle in the trident production process one has to integrate over spectrum of emitted photons. This means that both the mentioned mechanisms (contributing in the different parts of photon spectrum) should be taken into consideration and the developed approach is very suitable for solution of the problem.

One has to consider two different contributions into the probability of the process. The first one is the direct(one-step) electroproduction of pair via the virtual intermediate photon. The second one is the cascade(two-step) process when an electron emits the real photon moving in the field of axis and afterwards the photon converts into the pair. The interrelation of these contributions depends on the target thickness l since the probability of the direct process is proportional to l while the probability of the cascade process is proportional to $l^2/2$. In oriented crystals the real photon emission is strongly enhanced.

The electroproduction process in the oriented germanium crystal was studied recently in the experiment NA63 at SPS at CERN (for proposal see

[9]). The electroproduction process in an amorphous medium was considered recently by authors [5].

The direct process is considered in Sec.2. The cascade process is studied in Sec.3. The summary contribution of both processes is analyzed in Sec.4 using various approaches and including the conditions of the NA63 experiment. It is shown in Sec.5 that the created positron spectrum in the case of not very high the initial electron energy $\varepsilon < 200$ GeV and for soft positrons depends very weakly on the quite large energy loss.

2 Direct process

The contribution of the direct process into the probability of electroproduction in an amorphous medium was considered in detail in [5]. It is shown that in a thin target this contribution can be the essential part of the probability and dominates under some conditions. In an oriented crystal due to the strong enhancement of real photon emission comparing with the virtual one the contribution of the direct process is relatively small and one can use the equivalent photon method having a sufficient accuracy. The equivalent photon spectrum with the crystal field taken into account can be written within the logarithmic accuracy in the form (compare with Eq.(7) in [5])

$$n_E(y, z) = \frac{\alpha}{\pi} \frac{1-y}{y} \left[\left(1 + \frac{y^2}{2(1-y)} \right) \ln \frac{Q_E^2(y, z)}{q_E^2} - 1 \right], \quad (1)$$

where

$$\begin{aligned} Q_E^2(y, z) &= \frac{m^2 \omega^2}{\varepsilon_+ \varepsilon_-} \left(1 + \frac{\varepsilon_+ \varepsilon_-}{\omega^2} \kappa \right)^{2/3} = \frac{m^2 y^2}{z(y-z)} \left(1 + \frac{z(y-z)}{y^2} \kappa \right)^{2/3}, \\ q_E^2 &= \frac{m^2 \omega^2}{\varepsilon(\varepsilon - \omega)} \left(1 + \frac{\varepsilon - \omega}{\omega} \chi \right)^{2/3} = \frac{m^2 y^2}{1-y} \left(1 + \frac{1-y}{y} \chi \right)^{2/3}, \\ \chi(\varepsilon) &= \frac{eE}{m^2} \frac{\varepsilon}{m}, \quad \kappa(\omega) = \frac{eE}{m^2} \frac{\omega}{m}, \quad y = \frac{\omega}{\varepsilon}, \quad z = \frac{\varepsilon_+}{\varepsilon}, \quad \kappa = y\chi, \end{aligned} \quad (2)$$

where E is the electric field of crystal axis(plane) transverse to the velocity vector, ε is the energy of the initial electron, $\varepsilon_+, \varepsilon_-$ are the energy of particles of the created pair, $\omega = \varepsilon_+ + \varepsilon_-$ is the photon energy. Here the appearance of the additional factors depending on the parameters χ and κ is connected with expansion of the characteristic angles in the pair creation block and in the equivalent photon emission block at large values of these parameters. This item is discussed in the book [1], Sec.6.2 and 6.3.

In an amorphous medium the characteristic momentum transfers are changed due to influence of the multiple scattering on the photon emission process (the Landau-Pomeranchuk-Migdal (LPM) effect). It is shown in [5] that, when one takes into account the contribution of photons emitted by an electron at fly in a target (boundary photons) and the change of the lower limit of momentum transfer q_{\min}^2 under influence of the LPM effect, the value of q_{\min}^2 is restored in the summary contribution: $q_{\min}^2 = m^2 y^2 / (1 - y)$. Similar situation occurs in an oriented crystal if one takes into consideration the radiation of boundary photons by an electron at fly in a crystal field. The spectral distribution of boundary photons emitted by an electron at fly in a homogeneous electric field was found in [6], [7]. In our notation this distribution with the logarithmic accuracy [6] has the form

$$\frac{dw_i}{dy} = \frac{\alpha}{\pi} \frac{1-y}{y} \left(1 + \frac{y^2}{2(1-y)} \right) \ln \left(1 + \frac{1-y}{y} \chi \right)^{2/3}. \quad (3)$$

Putting Eqs.(1) and (3) together one obtains

$$n_E(y, z) + \frac{dw_i}{dy} = \frac{\alpha}{\pi} \frac{1-y}{y} \left[\left(1 + \frac{y^2}{2(1-y)} \right) \times \left(\ln \frac{1}{\xi} + \frac{2}{3} \ln \left(1 + z \left(1 - \frac{z}{y} \right) \chi \right) \right) - 1 \right], \quad \xi = \frac{z(y-z)}{1-y}. \quad (4)$$

In the range of applicability of the equivalent photon method ($z \ll 1$) and for not very high energy of the initial electron when $z\chi(\varepsilon) = \chi(\varepsilon_+) \leq 1$ the summary spectral distribution can be presented as

$$\frac{dw_s}{dy} = \frac{\alpha}{\pi} \frac{1-y}{y} \left[\left(1 + \frac{y^2}{2(1-y)} \right) \ln \frac{1}{\xi} - 1 \right]. \quad (5)$$

3 Cascade process

Basing on Eqs.(16) and (17) of [3] (see also Eq.(7.135) in [1]) one get the general expression for the spectral distribution of particles created by a photon

$$\begin{aligned}
dW(\omega, y_p) &= \frac{\alpha m^2}{2\pi\omega} \frac{dy_p}{y_p(1-y_p)} \int_0^{x_0} \frac{dx}{x_0} G(x, y_p), \\
G(x, y_p) &= \int_0^\infty F(x, y_p, t) dt + s_3 \frac{\pi}{4}, \\
F(x, y_p, t) &= \text{Im} \left\{ e^{f_1(t)} [s_2 \nu_0^2 (1+ib) f_2(t) - s_3 f_3(t)] \right\}, \quad b = \frac{4\kappa_1^2}{\nu_0^2}, \quad y_p = \frac{\varepsilon_+}{\omega}, \\
f_1(t) &= (i-1)t + b(1+i)(f_2(t) - t), \quad f_2(t) = \frac{\sqrt{2}}{\nu_0} \tanh \frac{\nu_0 t}{\sqrt{2}}, \\
f_3(t) &= \frac{\sqrt{2}\nu_0}{\sinh(\sqrt{2}\nu_0 t)}, \tag{6}
\end{aligned}$$

where

$$s_2 = y_p^2 + (1-y_p)^2, \quad s_3 = 2y_p(1-y_p), \quad \nu_0^2 = 4y_p(1-y_p) \frac{\omega}{\omega_c(x)}, \quad \kappa_1 = y_p(1-y_p)\kappa(x). \tag{7}$$

The situation is considered when the electron angle of incidence ϑ_0 (the angle between electron momentum \mathbf{p} and the axis) is small $\vartheta_0 \ll V_0/m$. The axis potential (see Eq.(9.13) in [1]) is taken in the form

$$U(x) = V_0 \left[\ln \left(1 + \frac{1}{x+\eta} \right) - \ln \left(1 + \frac{1}{x_0+\eta} \right) \right], \tag{8}$$

where

$$x_0 = \frac{1}{\pi d n_a a_s^2}, \quad \eta_1 = \frac{2u_1^2}{a_s^2}, \quad x = \frac{\varrho^2}{a_s^2}, \tag{9}$$

Here ϱ is the distance from the axis, u_1 is the amplitude of thermal vibration, d is the mean distance between atoms forming the axis, a_s is the effective screening radius of the potential. The parameters in Eq.(8) were determined by means of fitting procedure, see Table 1.

The local value of the parameter $\kappa(x)$, which determines the probability of pair creation in the field Eq.(8), is

$$\begin{aligned}
\kappa(x) &= -\frac{dU(\varrho)}{d\varrho} \frac{\omega}{m^3} = 2\kappa_s f(x, \eta), \quad f(x, \eta) = \frac{\sqrt{x}}{(x+\eta)(x+\eta+1)}, \\
\kappa_s &= \frac{V_0\omega}{m^3 a_s} \equiv \frac{\omega}{\omega_s}. \tag{10}
\end{aligned}$$

Table 1. Parameters of the pair photoproduction and radiation processes in the tungsten crystal, axis $\langle 111 \rangle$ and the germanium crystal, axis $\langle 110 \rangle$ for two temperatures T ($\varepsilon_0 = \omega_0/4, \varepsilon_m = \omega_m, \varepsilon_s = \omega_s$)

Crystal	$T(\text{K})$	$V_0(\text{eV})$	x_0	η_1	η	$\omega_0(\text{GeV})$	$\varepsilon_m(\text{GeV})$	$\varepsilon_s(\text{GeV})$	h
W	293	417	39.7	0.108	0.115	29.7	14.35	34.8	0.348
W	100	355	35.7	0.0401	0.0313	12.25	8.10	43.1	0.612
Ge	293	110	15.5	0.125	0.119	592	88.4	210	0.235
Ge	100	114.5	19.8	0.064	0.0633	236	50.5	179	0.459

For an axial orientation of crystal the ratio of the atom density $n(\varrho)$ in the vicinity of an axis to the mean atom density n_a is (see [3])

$$\frac{n(x)}{n_a} = \xi(x) = \frac{x_0}{\eta_1} e^{-x/\eta_1}, \quad \omega_0 = \frac{\omega_e}{\xi(0)}, \quad \omega_e = 4\varepsilon_e = \frac{m}{4\pi Z^2 \alpha^2 \lambda_c^3 n_a L_0}. \quad (11)$$

The functions and values in Eqs.(6) and (7) are (see [8])

$$\begin{aligned} \omega_c(x) &= \frac{\omega_e(n_a)}{\xi(x)g_p(x)} = \frac{\omega_0}{g_p(x)} e^{x/\eta_1}, \quad L = L_0 g_p(x), \quad L_0 = \ln(ma) + \frac{1}{2} - f(Z\alpha), \\ g_p(x) &= g_{p0} + \frac{1}{6L_0} \left[\ln(1 + \kappa_1^2) + \frac{6D_p \kappa_1^2}{12 + \kappa_1^2} \right], \quad g_{p0} = 1 - \frac{1}{L_0} \left[\frac{1}{42} + h\left(\frac{u_1^2}{a^2}\right) \right], \\ h(z) &= -\frac{1}{2} [1 + (1+z)e^z \text{Ei}(-z)], \quad a = \frac{111Z^{-1/3}}{m}. \end{aligned} \quad (12)$$

Here the function $g_p(x)$ determines the effective logarithm using the interpolation procedure, $D_p = D_{sc} - 10/21 = 1.8246$, $D_{sc} = 2.3008$ is the constant entering in the radiation spectrum at $\chi/u \gg 1$ (or in the positron spectrum in the pair creation process at $\kappa_1 \gg 1$), see Eq.(7.107) in [1], $\text{Ei}(z)$ is the integral exponential function.

The expression for the spectral probability of radiation is connected with the spectral distribution Eq.(6) ($dW/dy = \omega dW/d\varepsilon$) by the standard QED substitution rules: $\varepsilon_+ \rightarrow -\varepsilon$, $\omega \rightarrow -\omega$, $\varepsilon_+^2 d\varepsilon_+ \rightarrow -\omega^2 d\omega$ and exchange $\omega_c(x) \rightarrow 4\varepsilon_c(x)$. As a result one has for the spectral intensity $dI = \omega dW$

$$\begin{aligned}
dW_r(\varepsilon, y) &= \frac{\alpha m^2}{2\pi\varepsilon} \frac{\omega dy}{1-y} \int_0^{x_0} \frac{dx}{x_0} G_r(x, y), \\
G_r(x, y) &= \int_0^\infty F_r(x, y, t) dt - r_3 \frac{\pi}{4}, \\
F_r(x, y, t) &= \text{Im} \left\{ e^{\varphi_1(t)} \left[r_2 \nu_{0r}^2 (1 + ib_r) f_2(t) + r_3 f_3(t) \right] \right\}, \quad b_r = \frac{4\chi^2(x)}{u^2 \nu_{0r}^2}, \\
y &= \frac{\omega}{\varepsilon}, \quad u = \frac{y}{1-y}, \quad \varphi_1(t) = (i-1)t + b_r(1+i)(f_2(t) - t), \quad (13)
\end{aligned}$$

where

$$\begin{aligned}
r_2 &= 1 + (1-y)^2, \quad r_3 = 2(1-y), \\
\nu_{0r}^2 &= \frac{1-y}{y} \frac{\varepsilon}{\varepsilon_c(x)}, \quad (14)
\end{aligned}$$

here the functions $f_2(t)$ and $f_3(t)$ are defined in Eq.(6). The local value of the parameter $\chi(x)$ which determines the radiation probability in the field Eq.(8) is

$$\chi(x) = -\frac{dU(\varrho)}{d\varrho} \frac{\varepsilon}{m^3} = 2\chi_s f(x, \eta), \quad \chi_s = \frac{V_0 \varepsilon}{m^3 a_s} \equiv \frac{\varepsilon}{\varepsilon_s}, \quad (15)$$

where $f(x)$ is defined in Eq.(10).

The functions and values in Eqs.(13) and (14) (see also Eqs.(11) and (12)) are

$$\begin{aligned}
\varepsilon_c(x) &= \frac{\varepsilon_e(n_a)}{\xi(x) g_r(x)} = \frac{\varepsilon_0}{g_r(x)} e^{x/\eta_1}, \\
g_r(x) &= g_{r0} + \frac{1}{6L_0} \left[\ln \left(1 + \frac{\chi^2(x)}{u^2} \right) + \frac{6D_r \chi^2(x)}{12u^2 + \chi^2(x)} \right], \\
g_{r0} &= 1 + \frac{1}{L_0} \left[\frac{1}{18} - h \left(\frac{u_1^2}{a^2} \right) \right], \quad (16)
\end{aligned}$$

where the function $g_r(x)$ determines the effective logarithm using the interpolation procedure: $L = L_0 g_r(x)$, see Eq.(12), $D_r = D_{sc} - 5/9 = 1.7452$.

The expressions for the radiation probability dW_r Eq.(13) and the pair creation probability dW Eq.(6) include both the coherent and incoherent

contributions as well as the influence of the multiple scattering (the LPM effect) on the photon emission process (see [8]) or the pair creation process (see [4]). The probability of the coherent radiation is the first term ($\nu_{0r}^2 = 0$) of the decomposition of Eq.(13) over ν_{0r}^2 and the probability of the coherent pair creation is the first term ($\nu_0^2 = 0$) of the decomposition of Eq.(6) over ν_0^2 . The probabilities of the incoherent process are the second term ($\propto \nu_0^2, \nu_{0r}^2$) of the mentioned decompositions (compare with Eq.(21.21) in [1]).

In the cascade process the initial electron with the energy ε emitted the photon with the energy ω which creates in turn the electron-positron pair with the energies $\varepsilon_+, \varepsilon_-, \omega = \varepsilon_+ + \varepsilon_-$. The probability of the cascade process (in $1/\text{cm}^2$) is

$$\frac{dW_c(z, \varepsilon)}{dz} = \int_z^1 \frac{dW_r(\varepsilon, y)}{dy} \frac{dW\left(y\varepsilon, \frac{z}{y}\right)}{dz} dy, \quad (17)$$

where $dW_r(\varepsilon, y)/dy$ is given in Eq.(13) and $dW(\omega, y_p)/dz$ is given in Eq.(6), $\omega = y\varepsilon, y_p = z/y$.

It is known that the intensity of radiation in an oriented crystal is strongly amplified comparing with the corresponding amorphous medium, e.g. in the oriented along axis $\langle 110 \rangle$ germanium crystal at the temperature $T = 293$ K the radiation length at electron energy $\varepsilon = 180$ GeV is 22 times shorter than in the amorphous germanium, see Sec.17 in [1]. The spectra of photons emitted from electrons with different energies in the oriented germanium are shown in Fig.1. The spectra have the wide maximum situated at $y = 0.05$ for

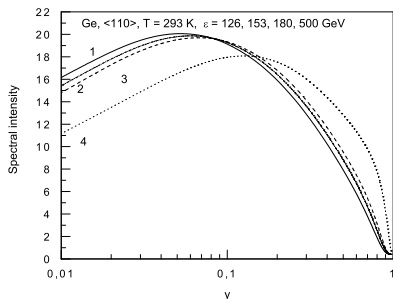


Fig. 1. The radiation spectral intensity vs the photon energy $y = \omega/\varepsilon$ in germanium, axis $\langle 110 \rangle$, temperature $T = 293$ K. The intensity distribution $dI(\varepsilon, y_r)/d\omega$ (in units cm^{-1}) The solid curve(1) is the theory prediction (see Eq.(13)) for the electron energy $\varepsilon = 126$ GeV, the dash-dot curve(2) is for the electron energy $\varepsilon = 153$ GeV, the dashed curve(3) is for the electron energy $\varepsilon = 180$ GeV, and the dotted curve(4) is for the electron energy $\varepsilon = 500$ GeV.

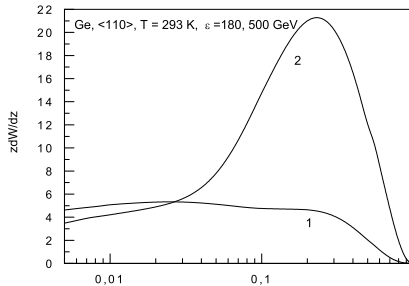


Fig. 2. The value $z dW_c^z(z, \varepsilon)/dz$ for the cascade pair electroproduction Eq.(17) in germanium, axis $\langle 110 \rangle$, temperature $T = 293$ K. The curves 1 and 2 are for the initial electron energy $\varepsilon = 180$ GeV and 500 GeV.

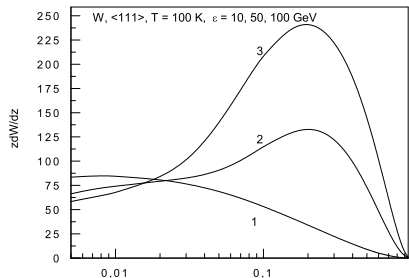


Fig. 3. The value $z dW_c^z(z, \varepsilon)/dz$ for the cascade pair electroproduction Eq.(17) in tungsten, axis $\langle 111 \rangle$, temperature $T = 100$ K. The curves 1, 2 and 3 are for the initial electron energy $\varepsilon = 10$ GeV, 50 GeV and 500 GeV.

$\varepsilon = 126$ GeV (the corresponding photon energy is $\omega_h = 6.3$ GeV), at $y = 0.06$ for $\varepsilon = 153$ GeV (the corresponding photon energy is $\omega_h = 9.2$ GeV), and at $y = 0.07$ for $\varepsilon = 180$ GeV (the corresponding photon energy is $\omega_h = 12.6$ GeV), while for $\varepsilon = 500$ GeV the maximum is situated at $y = 0.12$ and the corresponding photon energy is $\omega_h = 60$ GeV. The magnitudes of maxima for three first cases are very close to each other (the difference is less than 2%).

The emitted photons create the electron-positron pairs. Since the spectrum of created positron has overall drop $\sim 1/z$ it is instructive to plot the function $z dW_c/dz$ to trace details of the pair creation mechanism as it was done in [5]. The values of the function in the oriented along axis $\langle 110 \rangle$ germanium crystal at temperature $T = 293$ K are shown in Fig.2 for two energies $\varepsilon = 180$ GeV and 500 GeV. There are two mechanisms of pair creation by a photon in an oriented crystal: the coherent and the incoherent. When $\kappa_m \ll 1$ ($\kappa_m = \omega/\omega_m$, ω_m is contained in the Table 1) the incoherent mechanism of pair creation (weakly depending on the photon energy) dominates. Just this case exhibits the curve 1 and the left part of curve 2 in Fig.2. Starting from $\omega \simeq 2\omega_m/3$ the coherent mechanism comes into play (see e.g. the second term in Eq.(20) below, see also Fig.1 in [5]). Note that $2\omega_m/3 \simeq 60$ GeV is the position of the maximum at $\varepsilon = 500$ GeV in Fig.1. So the the large peak at the right part of curve 2 in Fig.2 is the coherent contribution.

The radiation spectra in the oriented along axis $\langle 111 \rangle$ tungsten crystal at temperature $T = 293$ K are shown in Fig.3 of [5]. The spectra have the wide maximum situated at $y = 0.003$ for $\varepsilon = 1$ GeV (the corresponding photon energy is $\omega_h = 3$ MeV), at $y = 0.009$ for $\varepsilon = 3$ GeV (the corresponding photon energy is $\omega_h = 27$ MeV), at $y = 0.01$ for $\varepsilon = 5$ GeV (the corresponding photon energy is $\omega_h = 50$ MeV), and at $y = 0.02$ for $\varepsilon = 10$ GeV (the corresponding photon energy is $\omega_h = 200$ MeV). The magnitudes of maxima for all four cases are very close to each other (the maximal difference is $\sim 2.5\%$). For higher electron energies the maximum is shifted to the right: for temperature $T = 100$ K it is at $y = 0.08$ for $\varepsilon = 50$ GeV (the corresponding photon energy is $\omega_h = 4$ GeV) and at $y = 0.1$ for $\varepsilon = 100$ GeV (the corresponding photon energy is $\omega_h = 10$ GeV)

The functions zdW_c/dz for cascade pair electroproduction in the indicated conditions in tungsten are shown in Fig.3 for three energies $\varepsilon = 10$ GeV, 50 GeV and 100 GeV. Since for $\varepsilon = 10$ GeV the maximum position $\omega_h \ll \omega_m \simeq 8$ GeV the incoherent mechanism of pair creation (weakly depending on the photon energy) dominates (the curve 1). The same remains true for the soft positron production at higher electron energies. The peaks at the right part of positron spectra for $\varepsilon = 100$ GeV and $\varepsilon = 50$ GeV situated at $z = 0.2$ are the contributions of the coherent radiation at the first stage of the process. For $\varepsilon = 100$ GeV the maximum position $\omega_h = 10$ GeV is twice of higher than $2\omega_m/3 \simeq 5$ GeV and the region of spectrum maximum contributes significantly (the curve 3), while for $\varepsilon = 50$ GeV $\omega_h = 4$ GeV is slightly less than $2\omega_m/3$ and the right part of the photon spectrum contributes only (the curve 2). This explains the sharp difference in heights of the peaks.

4 Summary probability of electroproduction

In the experiment NA63 carried out recently at SPS at CERN (for proposal see [9]) the electroproduction (trident production) process was studied in the oriented along axis $\langle 110 \rangle$ germanium crystal at temperature $T=293$ K. Targets with the thickness $l = 170 \mu\text{m}$ and $l = 400 \mu\text{m}$ were used. The theory prediction in the energy interval measured in NA63 is shown in Fig.4. The direct process contribution (in 1/cm) is

$$\frac{dW_d(z, \varepsilon)}{dz} = \int_z^1 \frac{dw_s(\varepsilon, y)}{dy} \frac{dW\left(y\varepsilon, \frac{z}{y}\right)}{dz} dy, \quad (18)$$

where $dw_s(z, \varepsilon)/dy$ is given in Eq.(5). The cascade process contribution (in $1/\text{cm}^2$) is defined in Eq.(17).

The summary contribution into the pair electroproduction probability of both the direct and the cascade mechanisms in an oriented crystal in the target with thickness l is

$$\frac{dW_S(z, \varepsilon)}{dz} = \frac{dW_d(z, \varepsilon)}{dz} l + \frac{dW_c(z, \varepsilon)}{dz} \frac{l^2}{2}. \quad (19)$$

The curve 1 in Fig.4 represents this summary contribution for $l = 400 \mu\text{m}$ while the curve 3 shows the same for $l = 170 \mu\text{m}$. The relative contribution of the direct process is maximal at the minimal positron energy $\varepsilon = 0.5 \text{ GeV}$. For $l = 170 \mu\text{m}$ the direct process contribution is $\sim 22\%$ of the cascade one while it is only $\sim 9\%$ for $l = 400 \mu\text{m}$. This relative contribution diminishes with the positron energy increase and at the positron energy $\varepsilon = 9 \text{ GeV}$ it becomes $\sim 7\%$ of the cascade contribution for $l = 170 \mu\text{m}$ and only $\sim 3\%$ for $l = 400 \mu\text{m}$.

It is customary to present the result in terms of the enhancement: the ratio of the electroproduction probability in an oriented crystal Eq.(19) to the corresponding probability in an amorphous medium [5]. The enhancement for two used thicknesses is shown in Fig.5. The increase of the enhancement with the positron energy growth for the given thickness is due to more fast decreasing of the probability in an amorphous medium. In the positron energy interval under consideration in an amorphous medium the main contribution into electroproduction probability gives direct process $\propto l$ (see Fig.2 in [5]), while in oriented crystal the cascade process probability $\propto l^2$ dominates. Because of this one has the higher enhancement for $l = 400 \mu\text{m}$.

We will discuss now an approximate approach to the consideration of pair electroproduction in the cascade process. The probability of the cascade process Eq.(17) depends on the probabilities of pair creation by a photon and photon emission from high-energy electron. The photon spectrum has the maximum in its soft part (e.g. in Ge $\omega_h = 12.6 \text{ GeV}$ for $\varepsilon = 180 \text{ GeV}$). From the other side it is known that for the pair creation process in germanium crystal the coherent (field) contribution becomes essential starting with the energy $\varepsilon = 50 \text{ GeV}$ (see Fig.2a in [8]). So one can expect that for $\varepsilon_+ \leq \varepsilon_m$ the main contribution in the pair creation part $dW(y\varepsilon, z/y)/dy$ gives the incoherent pair creation probability with the field (coherent) correction:

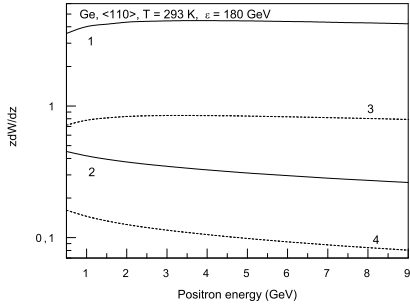


Fig. 4. The value $z dW_S/dz$ (see Eq.(19)) for the pair electroproduction in germanium. The curves 1 and 3 present the summary contribution into the pair electroproduction probability of both the direct and the cascade mechanisms in the oriented crystal (axis $\langle 110 \rangle$, $T = 293$ K) and the curves 2 and 4 show the summary contribution into the pair electroproduction probability of both the two-photon diagrams and the cascade process in an amorphous medium (see [5]) for $l = 400 \mu\text{m}$ and $l = 170 \mu\text{m}$, respectively. For convenience the ordinate is multiplied by 10^3 .

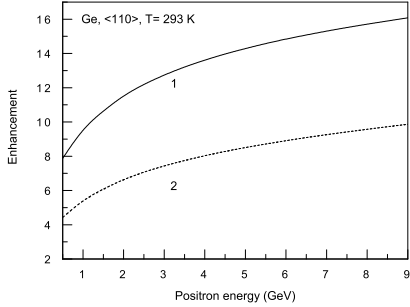


Fig. 5. The enhancement: the ratio of electroproduction probability in the germanium crystal axis $\langle 110 \rangle$, $T = 293$ K and the electroproduction probability in the amorphous germanium for the initial electron energy $\varepsilon = 180$ GeV. The curve 1 is for the target thickness $l = 400 \mu\text{m}$ and the curve 2 is for the target thickness $l = 170 \mu\text{m}$.

$$\frac{dW\left(y\varepsilon, \frac{z}{y}\right)}{dz} \rightarrow \frac{dW_{ic}(\varepsilon, z)}{dz} = \frac{g_{p0}}{yL_{rad}} \left(1 + \frac{1}{18L_0}\right)^{-1} \left[\left(1 - \frac{4z(y-z)}{3y^2}\right) + B \left(1 - \frac{z(y-z)}{y^2}\right) \exp\left(-\frac{2\varepsilon_m y}{3\varepsilon z(y-z)}\right) \right], \quad (20)$$

$$B = \frac{\pi\omega_0}{\eta_1\omega_m g_{p0}} \sqrt{-\frac{3f(x_m)}{4f''(x_m)}}, \quad x_m = \frac{1}{6} \left(\sqrt{1 + 16\eta(1 + \eta)} - 1 - 2\eta \right),$$

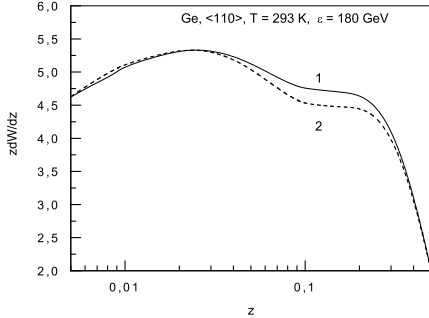


Fig. 6. The value $z dW_c/dz$ for the pair electroproduction in germanium. The curve 1 is calculated according to Eqs.(19), (17) and (18), while the curve 2 is calculated according to Eq.(19) and Eq.(20).

where L_{rad} is the Bethe-Maximon radiation length, see e.g. Eq.(7.54) in [1], and Eqs.(21.29) in the same book, the function $f(x)$ is defined in Eq.(10). Here the first term in r.h.s. is the Bethe-Maximon probability with crystal effects taken into account (g_{p0} is defined in Eq.(12)) and the second term is the field correction calculated according to Eq.(12.14) in [1] which is valid near the threshold of pair creation by a photon in the field. For considered cases in germanium $B = 24.5$ and in tungsten $B = 6.16$. The result of calculation of the cascade electroproduction probability is given in Fig.6. The curve 1 is the probability of the process according to Eq.(17) and the curve 2 is for the case when the pair creation probability is used in form Eq.(20). The maximal difference between the curves is 5% only (at $z = 0.15$). It should be noted that the coherent pair creation contribution (the second term in Eq.(20)) gives negligible contribution at $z \leq 0.05$, gives 7% of total contribution at $z = 0.1$ and is nearly half of total contribution at $z = 0.5$.

The main contribution into the spectrum of low energy positrons $z \ll 1$ gives soft photons $y \sim z \ll 1$. If the condition $x_0^{-3/2} \ll y/\chi_s \ll 1$ is fulfilled one can use Eqs.(17.11)-(17.13) in [1] for the description of the spectrum of emitted photons. The approximate spectral intensity distribution can be presented in the form

$$y \frac{dW_a(y)}{dy} = \frac{dI_a}{d\omega} = \frac{A}{L_{rad}} \left(\frac{y}{\chi_s} \right)^{1/3} g_1(y, \eta), \quad (21)$$

where

$$\begin{aligned}
 A &= \left(\frac{2}{\sqrt{3}}\right)^{5/3} \Gamma\left(\frac{2}{3}\right) \frac{\omega_0}{\eta_1 \varepsilon_s}, \quad g_1(y, \eta) = \ln \frac{\chi_s}{y} + a(\eta), \\
 a(\eta) &= \ln(18\sqrt{3}) - \frac{\pi}{2\sqrt{3}} - C - \frac{3}{4} - l_1(\eta), \quad C = 0.577\dots, \\
 l_1(\eta) &= \frac{3}{2} \int_0^\infty \left(f^{2/3}(x, 0) - f^{2/3}(x, \eta)\right) dx. \tag{22}
 \end{aligned}$$

Here the function $f(x, \eta)$ is defined in Eq.(10), the parameter χ_s is defined in Eq.(15).

The spectral intensity Eq.(21), which describes the radiation in the crystal field (the coherent radiation), is in quite satisfactory agreement with the spectral curves in Fig.1 not far from maximum. The incoherent contribution in the considered photon energy interval are damped as $(y/\chi_m)^{2/3}$ ($\chi_m = \varepsilon/\varepsilon_m$) comparing with the amorphous medium (see Eq.(21.23) in [1]). The LPM effect is damped more stronger. In the integral over the variable x , which defined the function $g_1(y, \eta)$, the large values x contributed up to $x \sim \chi_s/y$. For very soft photons $y \leq \chi_s/x_0^{3/2}$ all the interval $0 \leq x \leq x_0$ contributes. In the limiting case $y \ll \chi_s/x_0^{3/2}$ one has

$$y \frac{dW_a(y)}{dy} = \frac{dI_a}{d\omega} = \frac{A}{L_{rad}} \left(\frac{y}{\chi_s}\right)^{1/3} g_2(y, \eta), \tag{23}$$

where

$$\begin{aligned}
 g_2(y, \eta) &= \frac{3}{2} \int_0^{x_0} f^{2/3}(x, \eta) dx \simeq \frac{3}{2} \int_0^{x_0} f^{2/3}(x, 0) dx - l_1(\eta) \\
 &\simeq \frac{3}{2} \ln x_0 + \frac{9}{4} \ln 3 - \frac{\pi\sqrt{3}}{4} - l_1(\eta). \tag{24}
 \end{aligned}$$

One can calculate the probability of the electroproduction process substituting the probabilities Eq.(21) and Eq.(20) into Eq.(17). For $z \leq 0.1$ the obtained probability is 20%-30% higher than the direct calculation of Eq.(17). This is due to the fact that the whole spectrum of emitted photons (not only the vicinity of the maximum) is contributed into the final electroproduction probability and the tails of the curve Eq.(21) are higher than the spectrum Eq.(13).

The exact calculation of Eq.(17), which is the 5-fold integral, is quite cumbersome. We used the interpolated photon spectrum (the accuracy of interpolation is better than 1%) to simplify the calculation. When one uses the explicit expression Eq.(20) for the pair photoproduction probability, one can calculate the 3-fold integral directly. For the initial electron energy $\varepsilon < 200$ GeV the accuracy of the result is quite satisfactory. The simplest calculation (the 1-fold integral) is with use of the probabilities Eq.(21) and Eq.(20), but the result can be considered as a rough approximation only.

5 Conclusion

The process of the electroproduction of electron-positron pair (the trident production) in an oriented crystal is considered for the first time. It is shown that due to the strong enhancement of photon emission in an oriented crystal (this is the coherent radiation, see Fig.1) the electroproduction probability is also enhanced (see Fig.5). The scale of the enhancement in the soft part of created particles spectrum ($z \ll 1$) is similar to the photon emission enhancement. This is connected with the fact that in this part of the spectrum the standard incoherent (Bethe-Maximon) mechanism of pair creation by a photon (which is weakly dependent on photon energy) dominates (see e.g. Eq.(20)). For very high energy of incident electron ($\varepsilon > \varepsilon_m$) there is an additional enhancement in the hard part of created particles spectrum due to the coherent pair creation mechanism (see curve 2 in Fig.2). Indeed the enhancement E_c of the cascade process (the ratio of the electroproduction probability in the germanium crystal, axis $\langle 110 \rangle$, $T = 293$ K and of the electroproduction probability in the amorphous germanium) for the initial electron energy $\varepsilon = 500$ GeV attains $E_c \simeq 430$ at $z = 0.35$. This is because the both factors of the enhancement are acting: the coherent radiation ~ 20 and the coherent pair creation ~ 20 .

The similar situation occurs in the tungsten crystal. All the curves in Fig.3 are close to each other at $z \simeq 0.02$. At this value of z the enhancement of the cascade process $E_c \simeq 20$. For peak values at $z = 0.2$ one has $E_c \simeq 100$ at $\varepsilon = 100$ GeV. This is because the both factors of the enhancement are acting: the coherent radiation ~ 10 and the coherent pair creation ~ 10 . From the other side $E_c \simeq 54$ at $\varepsilon = 50$ GeV. This is because the coherent pair creation is not acting entirely at this electron energy as it was explained above.

In the germanium crystal (axis $\langle 110 \rangle$, $T = 293$ K) due to the action of the coherent mechanism of photon emission the crystal radiation length is

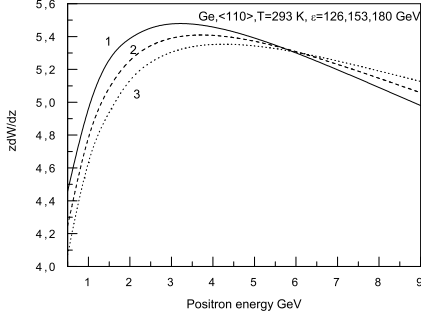


Fig. 7. The value $z dW_c/dz$ for the pair electroproduction in germanium. The curve 1 is for the initial electron energy $\varepsilon = 126$ GeV, the curve 2 is for $\varepsilon = 153$ GeV, the curve 3 is for $\varepsilon = 180$ GeV.

$L_{ch} = 1.02$ mm for the energy $\varepsilon = 180$ GeV. So the targets used in CERN experiment consist 40% and 17% of the crystal radiation length L_{ch} and the energy loss of the incident electron should be analyzed. Using the approach developed in [4] one can calculate the energy loss. For the initial energy $\varepsilon = 180$ GeV one has the final energy $\varepsilon_f = 153$ GeV for the target thickness $l = 170 \mu\text{m}$ and for the target thickness $l = 400 \mu\text{m}$ the final energy $\varepsilon_f = 126$ GeV. So the energy loss is very essential. However, the radiation spectra for these electron energies (shown in Fig.1) are very close to each other as it was indicated above. Since for electron energy $\varepsilon \leq 200$ GeV and for $z \ll 1$ the incoherent pair creation gives the main contribution, one can expect that the influence of the energy loss on the created positron spectrum will be quite weak. The positron spectra for corresponding electron energies are shown in Fig.7. The maximal difference (for the positron energy $\varepsilon_+ = 0.5$ GeV) is 8.6%. Taking into account the weak dependence of the positron spectrum on the initial electron energy one can use the average energy $\varepsilon_a = (\varepsilon + \varepsilon_f)/2$ for estimation of electron energy inside the targets. For the target thickness $l = 400 \mu\text{m}$ one has $\varepsilon_a = 153$ GeV and the influence of the energy loss will be $\sim 4\%$ for this thickness at $\varepsilon_+ = 0.5$ GeV and smaller (up to 0) at the higher positron energies ($\varepsilon_+ \leq 10$ GeV). For the target thickness $l = 170 \mu\text{m}$ the influence will be $\sim 2\%$ at $\varepsilon_+ = 0.5$ GeV and correspondingly smaller at higher positron energies. So we arrive to the paradoxical conclusion: in spite of essential energy loss by the initial electron in the targets the created positron spectrum depends very weakly on the energy loss in the case of not very high electron energy $\varepsilon < 200$ GeV and $z \ll 1$.

Acknowledgments

The authors are indebted to the Russian Foundation for Basic Research supported in part this research by Grant 06-02-16226.

References

- [1] V. N. Baier, V. M. Katkov and V. M. Strakhovenko, *Electromagnetic Processes at High Energies in Oriented Single Crystals*, World Scientific Publishing Co, Singapore, 1998.
- [2] V. N. Baier, V. M. Katkov and V. M. Strakhovenko, Nucl.Instr.and Meth, B 27 (1987) 360.
- [3] V. N. Baier, and V. M. Katkov, Phys.Lett., A 346 (2005) 359.
- [4] V. N. Baier, and V. M. Katkov, Phys.Lett., A 353 (2006) 91.
- [5] V. N. Baier and V. M. Katkov, Pis'ma v ZhETP, **88** (2008) 88.
- [6] M. Jacob, T, T, Wu, Phys.Lett. B 197 (1987) 253.
- [7] V. N. Baier, V. M. Katkov and V. M. Strakhovenko, Nucl. Phys. B 328 (1989) 387.
- [8] V. N. Baier, and V. M. Katkov, Phys.Lett., A 372 (2008) 2904.
- [9] J. U. Andersen, K.Kirsebom, S. P. Moller *et al*, *Electromagnetic Processes in Strong Crystalline Fields*, CERN-SPSC-2005-030.

V.N. Baier and V.M. Katkov

**Electroproduction of electron-positron pair
in oriented crystal at high energy**

В.Н. Байер, В.М. Катков

**Электророждение электрон-позитронной пары
в ориентированном кристалле при высокой энергии**

Budker INP 2008-28

Ответственный за выпуск А.М. Кудрявцев

Работа поступила 8.10.2008 г.

Сдано в набор 14.10.2008 г.

Подписано в печать 15.11.2008 г.

Формат бумаги 60×90 1/16 Объем 1.1 печ.л., 0.9 уч.-издл.

Тираж 105 экз. Бесплатно. Заказ № 28

Обработано на IBM PC и отпечатано на
ротапринте ИЯФ им. Г.И. Будкера СО РАН

Новосибирск, 630090, пр. академика Лаврентьева, 11.